Roll and Height Control for Legged Locomotion on the Water Surface

Nitish Thatte, Mahdi Khoramshahi, and Jason Rebello

Abstract— **Previous work on a biologically-inspired quadrupedal water runner robot demonstrated successful stabilization of robot pitch motions through the use of a passive tail. However, no method for controlling roll motions or robot height has been proposed. This paper presents an approach for controlling the roll and height of legged robots running on the water surface. First, we develop a simple model for water surface legged locomotion dynamics that maps leg velocities to forces. We then formulate an inverse dynamics control strategy based on this model that produces leg velocities in order to regulate the robot's height and roll angle. This control strategy is then applied to a detailed model of the water runner robot, and simulated experimental results are reported.**

I. INTRODUCTION

The Basilisk Lizard's striking ability to sustain highly dynamic legged locomotion on a range of surfaces from hard-ground to water is a remarkable feat [1]. Most legged robots would have difficulty emulating this animal's ability to robustly locomote on yielding or deforming surfaces. Therefore, to explore the dynamics of legged locomotion in this regime, we are studying the design of a bio-inspired water-running robot. Analyzing water-running dynamics may also help us gain insight into mobility on other yielding surfaces, such as granular media and mud. It is crucial that we develop locomotion models for these surfaces as robots continue to venture out of the laboratory and into the real world.

Previous works, [1], [2], [3], have considered the coupled vertical and horizontal kinematics and dynamics of the basilisk lizard. These works find that the Basilisk Lizard produces lift and thrust by cycling its feet through the water in three distinct phases: slap, stroke, and recovery. In the slap and stroke phases, the lizard generates vertical and horizontal forces primarily via fluid drag on the foot. Then, during the retraction phase, the lizard withdraws its foot within the air cavity produced during the previous phases, thereby greatly reducing overall downwards forces.

Based on this locomotion strategy a Park et al. designed and tested a bio-inspired water running robot. The robot could generate sufficient lift forces, but was unstable in roll and pitch [4]. Undesired pitching motion was remedied by adding a tail that generates a balancing moment via fluid drag forces as the robot moves forward. However, this work proposed no method for controlling the roll or the height of the robot. Therefore, in this paper, we seek to model the dynamics of the water runner robot so that we can develop a controller to stabilize these degrees of freedom.

II. LEGGED LOCOMOTION MODEL

A. Model Reduction

The cited studies provide detailed and complex descriptions of generated forces and dynamics during water surface locomotion. Specifically, complexity in these models arise from the hybrid dynamics imposed by the water contact discontinuity, the nonlinearity of drag forces and the curse of dimensionality. For the purposes of controller design, the complexity of previously developed models for water surface locomotion may limit intuition, provide more information than is necessary to accomplish the desired task, and preclude the development of analytic expressions for generated force and robot state. Therefore, to simplify and focus our analysis on the dynamics required to understand the height and roll motions, we will only consider vertical dynamics produced by a simplified foot trajectory in the following analysis.

Figure 1a shows the foot trajectory and the corresponding phase portrait of the previously built water runner robot [4]. In contrast, figure 1b shows a simplified circular foot trajectory and its corresponding phase diagram. We can see from the phase diagrams of the two trajectories that, especially during the plunge and stroke stages, the y-kinematics of the simplified foot trajectory and the actual foot trajectory are quite similar. This suggests that the y-dynamics produced by these two trajectories may also be similar.

Because we are neglecting the horizontal kinematics of the system, the circular foot trajectory can be further

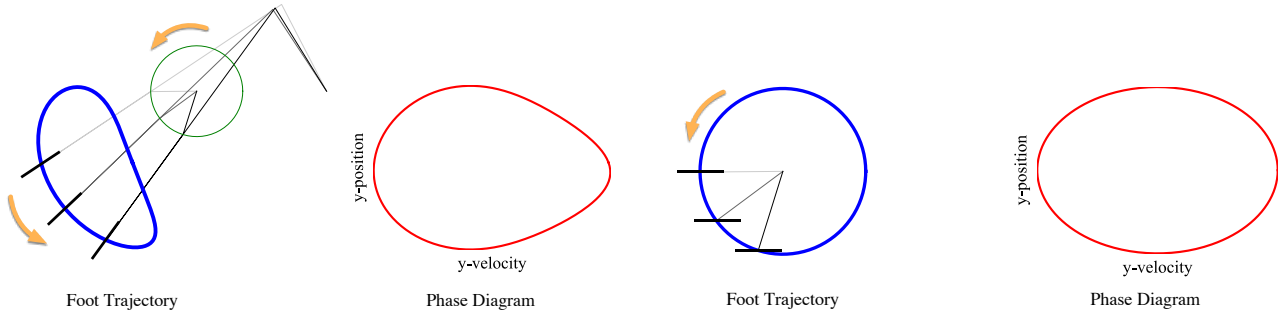

(a) The water runner robot's foot locus in blue, with three instantaneous configurations of the leg's four-bar mechanism shown in grey. The circular path traced by the joint at the end of the input link is traced in green. In red is the phase diagram of this legged system.

(b) A simplified circular foot locus in blue, with three instantaneous leg configurations shown in grey. In red is the phase diagram of this model.

Fig. 1: Trajectories and phase portraits for the water runner robot and a simplified model. Note that the orientation of the foot pad of the actual robot follows the orientation of the leg, whereas the orientation of the foot pad in the simplified mode is constant.

simplified to a foot mounted on a prismatic joint traveling vertically. We can calculate the force generated by a foot traveling on this trajectory via the equation obtained by Galsheen and McMahon [5], which states that the time-varying forces exerted by water during vertical impact of disks follows,

$$F(t) = -C_D^* \left[\frac{1}{2} S\rho \dot{y}_f(t) |\dot{y}_f(t)| + S\rho g y_f(t) \right] \quad (1)$$

where $F(t)$ is the time varying drag force, $C_D^* \approx 0.703$ is the drag coefficient, ρ is the density of water, g is the acceleration due to gravity, S is the effective circular area of the disk, and $y_f(t)$ and $\dot{y}_f(t)$ are the time-varying vertical position and velocity of the disk measured in a coordinate system where positive y opposes the gravity vector.

We can write the vertical dynamics of a one legged hopping robot as in figure 1b as the following system of differential equations:

$$\frac{d}{dt} \begin{bmatrix} y(t) \\ \dot{y}(t) \end{bmatrix} = \begin{bmatrix} \dot{y}(t) \\ \frac{1}{m} F(y(t), \dot{y}(t), \omega) - g \end{bmatrix} \quad (2)$$

Where $y(t)$ and $\dot{y}(t)$ are the position and velocity of the robot and ω is the frequency of the leg cycle.

In order to solve for the dynamics of the system we must reduce some of the complexity outlined earlier, First, to deal with the hybrid nature of the system, we will consider the average force generated in one leg cycle instead of the continuously varying force generated by the footpad. Next, we can deal with the curse of dimensionality by assuming that the velocity of the robot body oscillations are much less than the velocity of foot oscillations. This assumption is justified given the high operational frequency range of the robot (7 - 12 Hz), the quadratic damping of the water, and the relative masses of the robot body and the footpad. This assumption implies that the velocity of the footpad is a function of only the frequency of leg cycles, ω, and does not depend on the robot velocity.

Equation 1 shows that the magnitude of the force has a quadratic dependence on foot pad speed. Consequently, the robot should generate significantly more lift by plunging its foot into the water faster than it retracts its foot. Therefore, we can split the rotational speed of the robot into two parts, a downwards speed ω_1 and an upwards speed ω_2

We can now develop an expression for F_{avg} given y, $\dot{y}$, ω_1 and ω_2. First we define several constants: The drag coefficient of the water impact force is $b = \frac{1}{2} C_d S\rho$, the stiffness coefficient of the water impact force is $k = C_d S\rho g$, the height of the center of the foot trajectory with respect to the water is h, the amplitude of the foot oscillation is A, and the reduction in forces during the upwards part of the trajectory due to the air cavity and folding foot designs is α. The average force on the foot over one cycle is found by integrating equation 1 and dividing by the total time and is,

$$F_{avg} = \frac{\omega_1^2\omega_2}{\omega_1+\omega_2}\left[\frac{b}{2\pi}\left(A^2\arccos\frac{h}{A} - h\sqrt{A^2-h^2}\right)\right] - \frac{\alpha\omega_1\omega^2}{\omega_1+\omega_2}\left[\frac{b}{2\pi}\left(A^2\arccos\frac{h}{A} - h\sqrt{A^2-h^2}\right)\right] + \frac{\omega_2}{\omega_1+\omega_1}\left[\frac{k}{\pi}\sqrt{A^2-h^2} - h\arccos\frac{h}{A}\right] + \frac{\alpha\omega_1}{\omega_1+\omega_1}\left[\frac{k}{\pi}\sqrt{A^2-h^2} - h\arccos\frac{h}{A}\right] \quad (3)$$

B. Four Legged Model

To obtain a tractable model of the dynamics of a quadrupedal water runner robot, we can linearize the above equation about a nominal height and a roll angle of zero, as well as the expected leg frequency at this nominal height (obtained by solving equation 3 for ω such that $F_{avg} - mg = 0$). Linearization allows us to write the force generated by one foot in the form

$$F = G + A_y y + A_\theta\theta + B_1\omega_1 + B_2\omega_2 \quad (4)$$

Where G is the state and input independent forces such as gravitational forces, $A_y y$ is the height dependent force, $A_\theta\theta$ is the roll angle dependent forces, and $B_{\omega_1}\omega_1$ and $B_{\omega_2}\omega_2$ are the input dependent forces.

We can then combine the linearized forces and torques produced by each leg to write the linearized dynamics of the robot in the form

$$M\ddot{\vec{y}} = A\vec{y} + G + B\vec{\omega} \quad (5)$$

Where $\vec{y} = [y,\ \theta]^T$, is the output of the system and $\omega = [\omega_1^L\ \omega_1^R\ \omega_2^L\ \omega_2^R]^T$ is a vector of the left and right, upwards and downwards leg cycle frequencies.

III. CONTROLLER DESIGN

There are many possible techniques we can use to control the linear dynamical system given by equation 5. We choose to use a virtual model combined with an inverse dynamics approach so that we can directly solve for the four leg frequencies that produce desired accelerations. Because our dynamics matrix B is underdetermined, we can then use the nullspace of the dynamics matrix to consider other objectives and perform task prioritization.

We specify our desired behavior using a virtual model with a spring, damper, and integrator between the current and desired output:

$$\begin{aligned}\ddot{\vec{y}} &= K_p(\vec{y}_{des} - \vec{y}) + K_i\int_0^t(\vec{y}_{des} - \vec{y})d\tau \\ &\quad + K_d\frac{d}{dt}(\vec{y}_{des} - \vec{y}) \\ &= K_p\vec{e} + K_i\int_0^t\vec{e}d\tau + K_d\frac{d}{dt}\vec{e}\end{aligned} \quad (6)$$

Plugging equation 6 into equation 5 and solving for $\vec{\omega}$ gives our control law:

$$\vec{\omega} = B^\dagger\left[M\left(K_p\vec{e} + K_i\int_0^t\vec{e}d\tau + K_d\frac{d}{dt}\vec{e}\right) - A\vec{y} - G\right] + (\mathbb{1} - B^\dagger B)\vec{\omega}_0 \quad (7)$$

Where $B^\dagger$ is the psuedo-inverse of our dynamics matrix and $\mathbb{1}$ is the identity matrix. The term $(\mathbb{1} - B^\dagger B)\vec{\omega}_0$ projects $\vec{\omega}_0$ into the nullspace of our dynamics matrix. Therefore, the control inputs obtained by this control law will be as close to $\vec{\omega}_0$ as possible while providing our desired accelerations. As a result, we can use $\vec{\omega}_0$ to shape the control input to meet other desired objectives.

IV. RESULTS

We implemented the controller described in the previous section in order to regulate the height and roll of the water runner robot in simulation. To tune the gains on our virtual model, we used the Ziegler-Nichols Method as our virtual model is simply a PID controller in task-space. We assigned ω_0 by averaging the leg frequencies used in the last time step.

Figure 2a shows the closed and open-loop roll motion responses of the system subject to 1 Hz sinusoidal torques of various amplitude acting on the robot's center of mass in the roll direction. We do not show the height resposne, as the robot generally sinks only after reaching an extreme roll angle. It is evident from this figure that the controller is able to significantly reduce the effects of these disturbances on the robot as it is able to stabilize the robot against 2, 5, and 10 mN-m disturbances whereas the open loop system is unstable for all but the smallest amplitude disturbance. When we compare the responses of the system to the 2mN-m torque we see that the amplitude of osccilations is reduced in closed loop system.

Figure 2b shows the closed and open-loop responses of the system to sinusoidal disturbances with the same amplitudes as before, but at a a higher frequency of 2Hz. The open loop system fares better in this test, perhaps because the higher frequncy waves impose

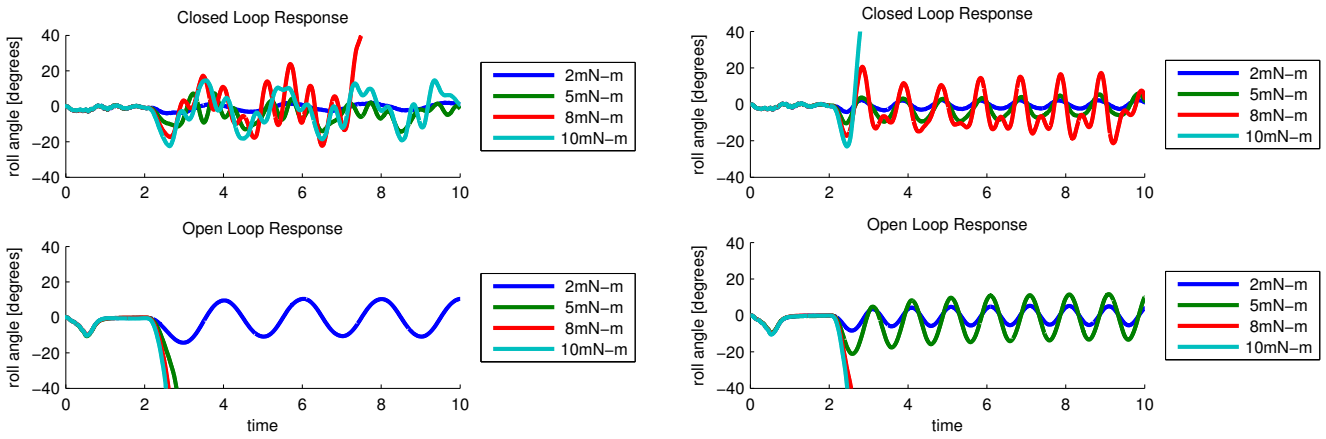

(a) 1 Hz

(b) 2 Hz

Fig. 2: Closed and open loop sytem response to sinusoidal disturbance torques at two frequencies and various amplitiudes. Disturbance starts at the two second mark.

smaller impulses on the system than the lower frequncy waves do. However, the performance of the closed loop system is still superior as, unlike the open loop system, it is stable against 8mN-m waves and it exhibits smaller oscillations than the open-loop system at disturbance frequencies for which both systems are stable.

V. CONCLUSIONS

In this work, we developed a linear model for the dynamics of a Water Running Robot, formulated an inverse dynamics controller based on this model, and demonstrated its effectiveness against sinusoidal disturbance torques in simulation. However, in order to truly gauge the performance of the controller, we must test it on a real robot. This step is crucial, as in there are a number of unmodeled complications that will arise during real-world testing. These include, but are not limited to, splashing and waves produced by the feet, motor dynamics, and sensor noise. Future work on the controller will address the issue of gait control using a central pattern generator or other techniques.

REFERENCES

[1] J. Glasheen and T. McMahon, "A hydrodynamic model of locomotion in the basilisk lizard," *Nature*, vol. 380, no. 6572, pp. 340–341, 1996.

[2] S. Floyd and M. Sitti, "Design and development of the lifting and propulsion mechanism for a biologically inspired water runner robot," *Robotics, IEEE Transactions on*, vol. 24, no. 3, pp. 698–709, 2008.

[3] S. T. Hsieh and G. V. Lauder, "Running on water: Three-dimensional force generation by basilisk lizards," *Proceedings of the National Academy of Sciences of the United States of America*, vol. 101, no. 48, pp. 16 784–16 788, 2004.

[4] H. S. Park, S. Floyd, and M. Sitti, "Roll and pitch motion analysis of a biologically inspired quadruped water runner robot," *The International Journal of Robotics Research*, vol. 29, no. 10, p. 1281, 2010.

[5] J. Glasheen and T. McMahon, "Vertical water entry of disks at low froude numbers," *Physics of Fluids*, vol. 8, p. 2078, 1996.